

Buffering the Aqueous Phase pH in Water-in-CO₂ Microemulsions

Justin D. Holmes,[†] Kirk J. Ziegler,[†] Mariska Audriani,[†] C. Ted Lee, Jr.,[†]
Prashant A. Bhargava,[†] David C. Steytler,[‡] and Keith P. Johnston^{*,†}

Department of Chemical Engineering, University of Texas at Austin, Austin, Texas 78712, and
School of Chemical Sciences, University of East Anglia, Norwich NR4 7TJ, U.K.

Received: March 3, 1999; In Final Form: April 30, 1999

The addition of organic and inorganic buffers to nanometer size water-in-CO₂ microemulsion droplets stabilized by ammonium perfluoropolyether (PFPE-NH₄) results in an increase in pH from 3 to values of 5–7. The effects of temperature, pressure, buffer type, buffer concentration, ionic strength, and CO₂ solubility on the pH inside water-in-CO₂ microemulsions and on biphasic water–CO₂ systems were measured by the hydrophilic indicator 4-nitrophenyl-2-sulfonate and were predicted accurately with thermodynamic models. In both systems, modest buffer loadings result in a steep pH “jump” from 2.5 pH units. Further increases in pH require large amounts of base to overcome buffering due to the carbonic acid–bicarbonate equilibrium. A pH approaching neutrality was obtained in w/c microemulsions with approximately 1.5 mol kg^{−1} NaOH. At high buffer loadings, the effects of temperature and pressure on pH values are negligible.

Introduction

Water-in-oil (w/o) microemulsions have been exploited for use in a wide range of applications, including chemical^{1–4} and enzymatic reactions,^{5–10} protein^{11–13} and metal extraction,¹⁴ and the production of nanoparticles.^{15–21} Microemulsions are attractive systems for studying such applications because they have the ability to function as a “universal” solvent medium by solubilizing high concentrations of both polar and apolar molecules within their dispersed aqueous and continuous oil phases, respectively. Amphiphilic molecules can also be adsorbed to the water–oil interface of the microemulsion droplets. Moreover, parameters such as water-pool size, surfactant concentration, and pH of the water-pool in w/o microemulsion can be readily tuned to purposefully alter the conditions in the system.

Further applications of microemulsions are presently being realized through the design of surfactants that stabilize water droplets in near critical and supercritical CO₂ (sc-CO₂), in the form of water-in-CO₂ microemulsions (w/c). CO₂ being nontoxic and nonflammable offers many environmental and safety advantages over conventional petrochemical solvents.²² Also, under the control of pressure and temperature, the density of sc-CO₂ can be readily manipulated, allowing for the selective separation of dissolved components. Surfactants that have been reported to stabilize w/c microemulsions include ammonium carboxylate perfluoroether surfactants (PFPE-NH₄),^{23–26} the hybrid hydrocarbon–fluorocarbon surfactant, C₇F₁₅CH(OSO₃[−]Na⁺)C₇H₁₅,²⁷ and the surfactant di(1*H*,1*H*,5*H*-octafluoro-*n*-pentyl) sodium sulfosuccinate (di-HCF₄).^{28–30} Water-in-CO₂ microemulsions have recently been exploited as reaction vessels due to the high miscibility of gaseous substrates in the CO₂ phase. Clarke et al.³¹ were able to solubilize ionic species in the water core of a w/c microemulsion and gaseous SO₂ and H₂S in the CO₂ phase to perform aqueous inorganic reactions.

Recently, Holmes et al.³⁰ reported the first enzymatic reactions undertaken in w/c microemulsions. In particular, linoleic acid was successfully bioconverted to a fatty acid by the enzyme soybean lipoxygenase dissolved in the aqueous phase, while the gaseous O₂ was mixed into the CO₂ phase.

The ability to perform reactions within the safe and tunable environment of a w/c microemulsion is clearly appealing. However, the usefulness of w/c microemulsions for both reaction and separation processes is limited because water in contact with CO₂ becomes acidic, pH ∼ 3, due to the formation and dissociation of carbonic acid,^{23,30,32} $\text{CO}_2 + \text{H}_2\text{O} \rightleftharpoons \text{H}_2\text{CO}_3 \rightleftharpoons \text{H}^+ + \text{HCO}_3^-$ (H⁺ exists in solution as H₃O⁺).

Many enzymes exhibit an optimum catalytic turnover of substrate at higher pH values and would be expected to perform at a much reduced activity in this acidic domain. For example, the enzyme *Chromobacterium viscosum* lipase displays its greatest activity at pH ∼ 6.5.³³ In the sc-CO₂ extraction of metal ions and ionizable organic species, control of the aqueous phase pH is essential.^{32,34} Holmes et al.³⁰ have previously reported on the problem of increasing the pH inside w/c microemulsions and biphasic water–CO₂ systems. Water droplets in a di-HCF₄-stabilized microemulsion were “buffered” with 100 mmol kg^{−1} 2-[*N*-morpholino]ethanesulfonic acid, sodium salt (MES), fixing the aqueous phase pH at around 5. In the biphasic system of bulk water and buffer, the pH of the aqueous phase could be raised to a pH beyond 6.

Henry’s law has been used previously to calculate the pH of a water phase in contact with CO₂ at elevated pressures.^{23,32,35} Benchmark CO₂ solubility studies were published by Weibe and Gaddy in the 1940s and more recently by King et al.^{36–38} Comparisons between direct measurement of the pH of water in contact with CO₂ using the spectroscopic pH probe bromophenol blue and theoretically predicted pH values have been reported by Toews et al.³² In unbuffered w/c microemulsions, Niemeyer and Bright observed that there was a mean difference between the experimentally determined and theoretically predicted pH values of approximately 0.5 pH units, using the

* To whom correspondence should be addressed. Telephone: (001) 512 471-4617. Fax: (001) 512 475-7824. E-mail: kpj@che.utexas.edu.

[†] University of Texas.

[‡] University of East Anglia.

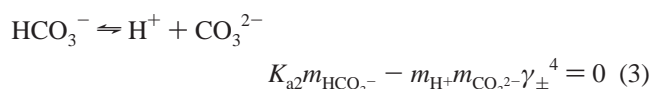
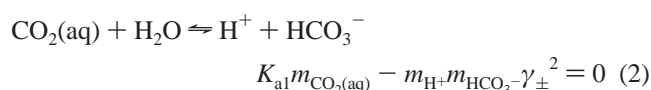
fluorescent probe Cl-NERF.²³ Hence, they postulated that the PFPE-NH₄ reverse micelles act as a partial barrier to CO₂.

In this current study, we examine the effectiveness of a variety of organic zwitterionic^{39–42} and inorganic buffers in raising the aqueous pH phase in both w/c microemulsions and two-phase water–CO₂ systems to values between 6 and 7. The pH of the coexisting water phase was monitored by the UV–vis absorption profile of the hydrophilic indicator 4-nitrophenyl-2-sulfonate (NPS).⁴³ There have been many debates about using optical probes to measure the pH within a reverse micelle water-pool, due to ionic strength effects resulting from the close proximity of highly charged surfactant headgroups.^{23,30,43–50} In this study, the effect of ionic strength on the behavior of the indicator has been accounted for and consequently the pH inside the dispersed phase of w/c microemulsions has been estimated. Theoretical models have been developed that predict the aqueous pH inside buffered PFPE-NH₄-stabilized microemulsions and biphasic water–CO₂ systems based on CO₂ solubility data published by Weibe and Gaddy.^{36,37}

Thermodynamic Prediction of pH for CO₂–Aqueous Systems

The dissociation of NPS in w/c microemulsions and biphasic water–CO₂ systems was studied. pH was determined from the molal concentration of hydrogen ions (m_{H^+}). The following reaction equilibria describe each of the buffer systems for a CO₂–aqueous “biphasic” pH model. The pH may be predicted for each biphasic system by using a Newton–Raphson method to solve a set of nonlinear equations.⁵¹

Biphasic Model. Pure Water–CO₂ System. The relevant equations for a binary solution of water and CO₂ includes the dissociation of water, the first and second dissociation of carbonic acid, and the dissociation of the indicator as described by the following equations:



where K_{a1} and K_{a2} are the first and second dissociation constants of carbonic acid given by Stumm and Morgan⁵² and m_{CO_2} refers to both CO₂(aq) and H₂CO₃. K_w is the ion product of water given by Marshall and Franck.⁵³ K_{NPSH} is the dissociation constant of the NPS and was determined experimentally in this study, 1.38×10^{-7} mol kg⁻¹ at 25 °C. It is assumed that the individual ionic activity coefficients, γ_k , are not sensitive to the specific individual properties of each ion and can be described by the mean ionic activity coefficient, γ_{\pm} .⁵⁴

$$\ln \gamma_{\pm} = -A_{\varphi} \left[\frac{\sqrt{I}}{1 + 1.2\sqrt{I}} + \frac{2}{1.2} \ln(1 + 1.2\sqrt{I}) \right] \quad (5)$$

where A_{φ} is the Debye–Huckel parameter⁵⁵ and I is the ionic strength for all species k with a charge z_k . For multiply charged species in solution, the following equation is used:⁵⁵

$$\ln \gamma_k = z_k^2 \ln \gamma_{\pm} \quad (6)$$

In addition, the “biphasic” model includes a charge balance and mass balance on the indicator (not shown) and CO₂:

$$m_{Na^+} + m_{H^+} - m_{HCO_3^-} - 2m_{CO_3^{2-}} - m_{OH^-} - m_{NPSH^-} - 2m_{NPS^{2-}} = 0 \quad (7)$$

$$m_{CO_2}^o - m_{CO_2(aq)} - m_{HCO_3^-} - m_{CO_3^{2-}} = 0 \quad (8)$$

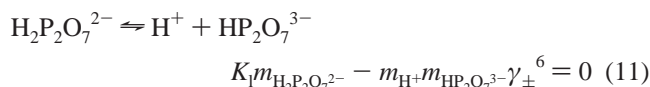
where $m_{CO_2}^o$ is the solubility of CO₂ in water at a given temperature and pressure and is assumed to be independent of salinity.^{36,37} The concentration of Na⁺ is known. The NaOH–water–CO₂ system is described by the same equations, but the concentration of Na⁺ is modified by the addition of NaOH.

NaHCO₃–Water–CO₂ System and Na₂CO₃–Water–CO₂ System. For these systems, the model uses eqs 1–7 and the CO₂ mass balance in eq 8 is replaced with the following to account for the addition of CO₂ from bicarbonate (eq 9) or carbonate (eq 10).

$$m_{CO_2}^o + m_{NaHCO_3}^o - m_{CO_2(aq)} - m_{HCO_3^-} - m_{CO_3^{2-}} = 0 \quad (9)$$

$$m_{CO_2}^o + m_{Na_2CO_3}^o - m_{CO_2(aq)} - m_{HCO_3^-} - m_{CO_3^{2-}} = 0 \quad (10)$$

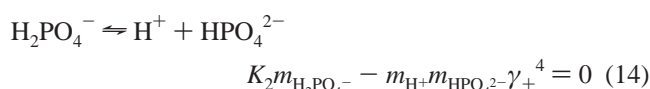
Pyrophosphate–Water–CO₂ System. This system includes eqs 1–8 and, in addition, a dissociation reaction for this buffer given by eq 11, a mass balance on the buffer, as well as changes in the charge balance. Only one dissociation reaction of pyrophosphate was considered due to the pK_a's of the other dissociation reactions.^{39,42}



$$m_{Na_4P_2O_7}^o - m_{HP_2O_7^{3-}} - m_{H_2P_2O_7^{2-}} = 0 \quad (12)$$

$$m_{Na^+} + m_{H^+} - m_{HCO_3^-} - 2m_{CO_3^{2-}} - m_{OH^-} - m_{NPSH^-} - 2m_{NPS^{2-}} - 3m_{HP_2O_7^{3-}} - 2m_{H_2P_2O_7^{2-}} = 0 \quad (13)$$

Phosphate–Water–CO₂ System. Similarly, this system includes eqs 1–8, a dissociation reaction for this buffer, a mass balance on the buffer, and a charge balance as follows:



$$m_{Na_2PO_4}^o - m_{HPO_4^{2-}} - m_{H_2PO_4^-} = 0 \quad (15)$$

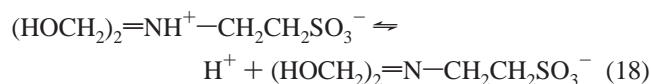
$$m_{Na^+} + m_{H^+} - m_{HCO_3^-} - 2m_{CO_3^{2-}} - m_{OH^-} - m_{NPSH^-} - 2m_{NPS^{2-}} - 2m_{HPO_4^{2-}} - m_{H_2PO_4^-} = 0 \quad (16)$$

Again, only one dissociation reaction was considered.^{39,42}

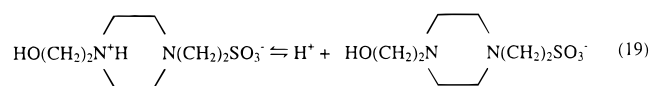
Organic Zwitterionic Buffer–Water–CO₂ System. Equations 1–8 are used along with a dissociation equation for the buffers given in eqs 18–23:

$$K_1m_{HB} - m_{H^+}m_{B^-}\gamma_{\pm}^2 = 0 \quad (17)$$

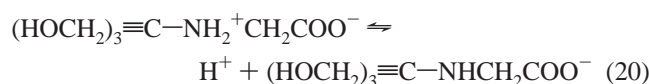
(a) *N,N*-Bis[2-hydroxyethyl]-2-aminoethanesulfonic acid, sodium salt (BES) dissociation:



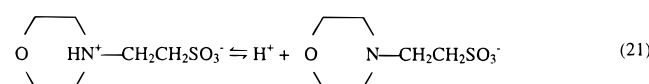
(b) *N*-[2-Hydroxyethyl]piperazine-*N'*-[2-ethanesulfonic acid], sodium salt (HEPES) dissociation:



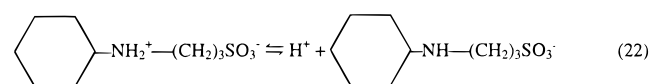
(c) *N*-Tris[hydroxymethyl]methylglycine (Tricine) dissociation:



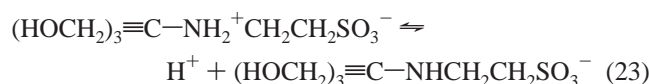
(d) 2-[*N*-Morpholino]ethanesulfonic acid, sodium salt (MES) dissociation:



(e) 3-[Cyclohexylamino]-1-propanesulfonic acid (CAPS):



(f) *N*-Tris[hydroxymethyl]methyl-2-aminosulfonic acid, sodium salt (TES):



A mass balance on the buffers is given in eq 24, and a charge balance in eq 25:

$$m_{\text{NaB}}^0 - m_{\text{HB}} - m_{\text{B}^-} = 0 \quad (24)$$

$$m_{\text{Na}^+} + m_{\text{H}^+} - m_{\text{HCO}_3^-} - 2m_{\text{CO}_3^{2-}} - m_{\text{OH}^-} - m_{\text{NPSH}^-} - 2m_{\text{NPS}^{2-}} - m_{\text{B}^-} = 0 \quad (25)$$

Experimental Section

Materials and Reagents. Perfluoropolyether carboxylic acid (PFPE-COOH) obtained from Ausimont was used as received; general formula $\text{F}_3\text{C}[(\text{OCF}_2\text{CF}(\text{CF}_3))_n(\text{OCF}_2)_m]\text{OCF}_2\text{COOH}$ ($n \approx 3$, $m \approx 2$), mass average molecular weight (M_w) = 665; lot number, D5. The ammonium carboxylate perfluoropolyether (PFPE-NH₄, M_w = 672) was prepared by stirring carboxylic acid (20 g, 30.35 mmol kg⁻¹) in 10 times molar excess of ammonium hydroxide (ACS reagent grade, Aldrich) for 24 h. Most of the ammonia and water was evaporated from the PFPE-NH₄ surfactant by stirring the solution in the fumehood for 24 h. Once the mixture became viscous the sample was dried in a vacuum oven at 25 °C for 48–72 h. Full conversion of the acid to the ammonium carboxylate was confirmed by FTIR spectroscopy:^{31,56,57} -COOH, 1775 cm⁻¹ (vs), -COO⁻NH₄⁺, 1656 cm⁻¹ (vs), NH₄⁺ ion, 3300–3030 cm⁻¹ (s). The water content of the surfactant dissolved in anhydrous methanol was 0.2 wt %, as determined by Karl–Fischer titration.⁵⁸

Deionized water was used in all experiments, and carbon dioxide (99%) was used as received (BOC gases). The buffers examined in this study, CAPS, Tricine, HEPES, TES, BES,

MES, anhydrous sodium carbonate (Na₂CO₃), anhydrous sodium bicarbonate (NaHCO₃), sodium pyrophosphate decahydrate (Na₄P₂O₇·10H₂O), sodium orthophosphate heptahydrate (Na₂HPO₄·7H₂O), and sodium hydroxide, were obtained from Sigma Chemical Co. (St. Louis, MO).

The hydrophilic pH indicator 4-nitrophenyl-2-sulfonate (NPS), C₆H₃NO₆SN₂, M_w = 263, was synthesized by direct sulfonation of 4-nitrophenol (C₆H₅NO₃, M_w = 139.1) based on a procedure outlined by Vogel et al.⁵⁹ The NPS crystals were characterized by chemical-ionization mass spectrometry and pulsed Fourier transform 100-MHz ¹H NMR: CI-MS (CH₄, 4 × 10⁻³ bar) m/z = 219, 241; ¹H NMR (D₂O) δ = 8.56 (doublet 3 H), δ = 8.0985 (quartet, 5 H), and δ = 6.5425 (doublet, 5 H).

Phase Behavior Measurements. A variable volume view cells (28 mL), with a sapphire front window for direct observation, was used to determine phase boundaries as described previously.⁶⁰ The maximum operating pressure of the cell is 345 bar, and accurate thermostating was achieved with a conventional bath-circulator (± 0.20 °C). An external magnetic stirrer drove a PTFE-coated magnetic stir bar.

To prepare a sample for study, PFPE-NH₄ (3 wt %) was added to the optical cell, followed by an aliquot of solution containing the selected buffer (w_0 = 20). A microprocessor-controlled high-pressure syringe pump (Isco, Model 260D, Lincoln, NE) was used to deliver CO₂ into the cell, and pressure was controlled to ± 0.2 bar. The cell was loaded with CO₂ at the experimental temperature, and the pressure was raised with the contents of the cell continuously stirred until a single-phase microemulsion was formed. The pressure–temperature phase stability profiles for the w/c microemulsions were determined by direct observation of turbidity accompanying phase separation. Such transitions, measured at constant temperature with decreasing pressure, are clearly visible and highly reproducible to within ± 4 bar.

pH Measurements. For spectroscopic measurements, a stainless steel batch cell of nominal volume (5.93 mL) was used.⁶⁰ The cell was fitted with two UV-grade sapphire windows, giving an optical path length of 1.72 cm. The maximum operating pressure of the cell is 345 bar. The cell was covered with heating tape (2 m) and thermostated to ± 0.2 °C by using a platinum resistance thermometer and a temperature controller. Pressure was controlled to ± 0.2 bar using a 60 mL syringe pump (High Pressure Equipment Co.). An external magnetic stirrer drove a PTFE-coated magnetic stir bar. For biphasic water–CO₂ mixtures an aqueous solution containing NPS (60 $\mu\text{mol kg}^{-1}$), and the appropriate buffer (5 mL) was introduced into the cell. The initial pH of the solution was adjusted to its pK_a . CO₂ was then added to the cell at a certain temperature and pressure, and the contents of the cell were stirred vigorously to ensure equilibrium between the two phases. For pH studies in w/c microemulsions the PFPE-NH₄ surfactant (3 wt %) and the buffered indicator (5 mmol kg⁻¹), w_0 = 20, were loaded into the cell. The sample for study was then prepared as described in the phase behavior measurements. All UV–vis spectra were recorded using a Cary 300 Series UV–vis dual beam spectrophotometer.

Results and Discussion

Determination of an Experimental pH Calibration Curve for NPS. The aqueous phase pH inside PFPE-NH₄-stabilized w/c microemulsions, at w_0 = 20, and biphasic water–CO₂ mixtures, was probed using the hydrophilic indicator NPS.^{30,43} The sulfonate moiety on NPS has an extremely low pK_a , ca. 1.5; consequently, only the charged acid (NPSH⁻) and conjugate

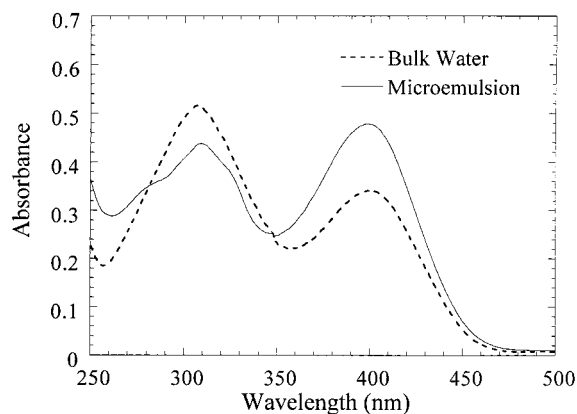


Figure 1. UV-visible absorbance spectra of 4-nitrophenyl-2-sulfonate in a HEPES-buffered w/c microemulsion at pH ~ 5.7 , $[\text{NPS}]_{\text{aq}} = 5 \text{ mmol kg}^{-1}$, and $[\text{HEPES}]_{\text{aq}} = 1.0 \text{ mol kg}^{-1}$, and in a bulk water phase at pH ~ 6.4 , $[\text{NPS}]_{\text{aq}} = 40 \text{ } \mu\text{mol kg}^{-1}$.

base (NPS^{2-}) forms of the indicator were present in the pH range studied. When hydrophilic indicators are used to measure the effective pH of water pools in microemulsions, the location of the indicator inside the reverse micelle needs to be established.^{43,44,61} Figure 1 shows the UV-vis absorbance spectrum of NPS in its acid and basic forms in bulk aqueous solution and a w/c microemulsion. The acid form of the indicator shows an absorption maximum at $\lambda = 308 \text{ nm}$ in bulk solution and $\lambda = 308 \text{ nm}$ in the w/c microemulsion. NPS^{2-} has a maximum absorption at $\lambda = 400 \text{ nm}$ in both the bulk solution and w/c microemulsion. Therefore, as observed in w/o microemulsions⁴³ both the acid and basic forms of NPS are confined to the aqueous domain in these w/c microemulsions. The molar extinction coefficients for NPSH^- and NPS^{2-} in bulk water were calculated to be 9.2×10^3 ($\lambda_{309\text{nm}}$) and 17×10^3 ($\lambda_{400\text{nm}}$) $\text{dm}^3 \text{ mol}^{-1} \text{ cm}^{-1}$, respectively. The pK_a of NPS in pure water was determined to be 6.86 ± 0.05 .

The effect of ionic strength on the acid-base behavior of NPS in the microemulsion also must be addressed when attempting to measure the pH of the dispersed phase. In an AOT reverse micelle, dissociated surfactant headgroups will contribute to the ionic strength of the dispersed droplet.⁴³ However, only 10–40% of AOT molecules in a reverse micelle are dissociated.^{44,61–64} Assuming that 25% of the PFPE- NH_4 molecules in the w/c reverse micelle are not bound to counterions, then the concentration of both the free NH_4^+ counterions and dissociated surfactant molecules in each water droplet is approximately 0.42 mol kg^{-1} . As the ionic strength in the water pool of the microemulsion increases, the stability of aqueous charged ions also increases due to a decrease in γ_{\pm} . Hence, reactions 2 and 3 are shifted toward the formation of carbonate ions and protons resulting in a lowering of the pH.

Figure 2 summarizes how the predicted pH of the water pool in a w/c microemulsion changes as a function of HEPES buffer concentration. The solid line presents the predicted pH values inside the w/c microemulsion using the “biphasic” model. The dashed line depicts how the pH values vary if 25% of the PFPE- NH_4 surfactant molecules in each microemulsion droplet dissociate to produce charged headgroups and free NH_4^+ counterions. At aqueous buffer loadings below 0.5 mol kg^{-1} , there is a noticeable difference resulting from the change in ionic strength. However, at the high buffer loadings used in this study ($0.5\text{--}1.5 \text{ mol kg}^{-1}$) pH values are only marginally affected by headgroup dissociation.

By establishing that NPS is located in the central water-pool of our w/c microemulsions, which at a $w_0 = 20$ have

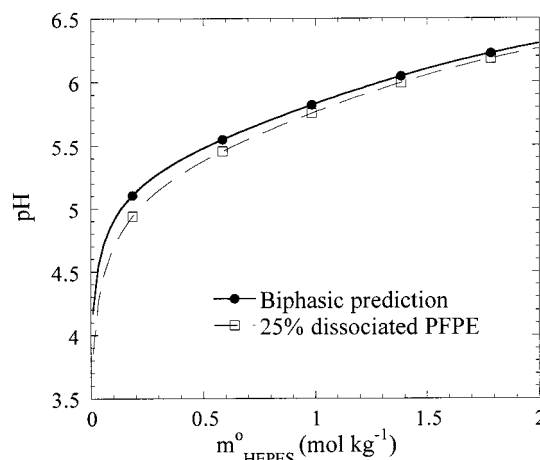


Figure 2. Predicted aqueous pH values inside a HEPES-buffered w/c microemulsion using the biphasic model and a modification of the biphasic model to account for 25% of the PFPE- NH_4 molecules being dissociated. $T = 35 \text{ }^\circ\text{C}$, $P = 345 \text{ bar}$.

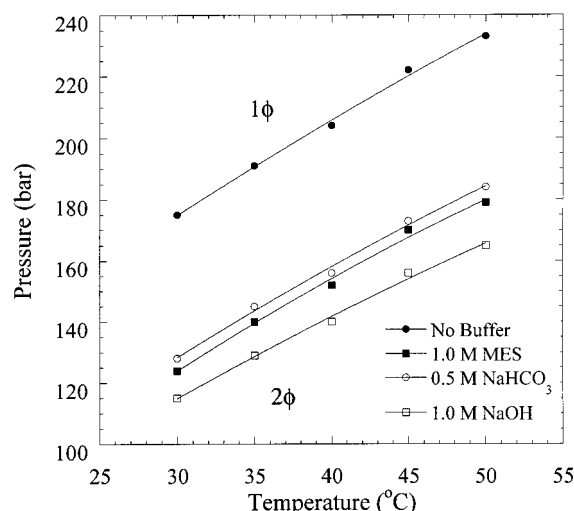


Figure 3. Pressure-temperature phase boundaries for a PFPE- NH_4 -stabilized w/c microemulsion, at $w_0 = 20$, in the absence and presence solubilized buffer. 1ϕ and 2ϕ represent single and two-phase regions. $[\text{PFPE-NH}_4] (M_w = 672) = 3 \text{ wt } \%$.

properties similar to those of bulklike water, and secondly that the ionic strength contribution from dissociated surfactant molecules is small at high buffer loadings, the pH in the aqueous phase of our w/c microemulsions can therefore be determined. The pH values of the aqueous phases of both biphasic systems and w/c microemulsions were obtained spectroscopically from eq 4 by comparing the UV-vis acid-base peak ratios of NPS to a calibration curve determined for a 1 mol kg^{-1} HEPES-buffered bulk solution containing NPS. A calibrated pH meter was used to accurately determine the pH of the HEPES-buffered solution at various NPS acid-base peak ratios.

Phase Behavior of Buffered Microemulsions. Figure 3 shows how the pressure-temperature phase boundary for the PFPE- NH_4 -stabilized w/c microemulsion changes with the addition of buffer. An increase in the ionic strength of the dispersed water phase results in a shift of the phase boundary to higher temperatures and lower pressures,^{65–68} as has been seen for water-in-ethane microemulsions.^{69,70} A lowering of the phase boundary was observed for all of the buffers studied. A reduction of the pressure phase boundary for PFPE- NH_4 w/c microemulsions, with the addition of $2.5\text{--}3.8 \text{ mol kg}^{-1}$ KBr,⁷¹ and for the di- HCF_4 -stabilized w/c microemulsions, with the addition of 100 mmol kg^{-1} MES, has previously been reported.³⁰

TABLE 1: Comparison of buffer solubilities in PFPE-NH₄-Stabilized Microemulsions and Bulk Water^a

buffer name	pK _a (20 °C) ^{38–41}	dpK _a /dT (°C ⁻¹) ^{38–41}	max. solubility of buffer in w/c microemulsion (mol kg ⁻¹)	solubility of buffer in bulk water (0 °C) ^{41,73} (mol kg ⁻¹)	theoretically predicted ionic strength in the w/c microemulsion
CAPS	10.4	-0.018	0.2		0.6
Na ₂ CO ₃	10.25	-0.009	0.5	0.67	1.6
Na ₃ P ₂ O ₆	8.2	-0.006	0.2	0.012	2.1
Tricine	8.15	-0.021	0.8	0.8	1.4
HEPES	7.5	-0.014	1.2	2.25	1.8
TES	7.4	-0.02	0.5	2.6	1.0
BES	7.1	-0.016	1.1	3.2	1.7
Na ₂ HPO ₄	6.8	-0.005	0.5	3.88	1.9
NaHCO ₃	6.3	-0.009	0.5	0.82	1.0
MES	6.15	-0.011	1.0	0.65	1.6
NaOH	14		1.5	10.5	2.7

^a The predicted aqueous ionic strengths at the maximum solubility of each buffer in the w/c microemulsions are also shown.

The lowering of the pressure phase boundary with increasing salinity can be explained by considering the stability of w/c microemulsions. SANS experiments have shown that for the PFPE-NH₄-stabilized microemulsion used in this study that there is no change in droplet structure as a function of pressure.²⁴ These SANS results suggest that microemulsion stability is dependent on interdroplet interactions rather than natural curvature.^{65,68} Using w/o microemulsions for reference, it is likely that increasing the salinity of the w/c microemulsion will result in the closer packing of the polar surfactant headgroups. Consequently, the interfacial region has more rigidity, resulting in a reduction in the degree of droplet interpenetration during collision and a lowering of the pressure phase boundary.^{65,69,70}

A unique feature of using the PFPE-NH₄ surfactant ($M_w = 672$) is that in CO₂, at a $w_0 = 20$, a high concentration of buffer can be loaded into the water pool. When a lower molecular weight surfactant ($M_w = 587$) was used to form the w/c microemulsion, a much lower buffer concentration could be solubilized into the water-pool, e.g., only 0.2 mol kg⁻¹ HEPES. Also, w/c microemulsions stabilized by this surfactant could only support a water loading around $w_0 \sim 15$. For these lower molecular weight PFPE-NH₄ microemulsions, stability becomes dependent on the natural curvature of the interfacial film separating the CO₂ phase from the water phase. For w/o systems where stability is determined by natural curvature, the solubilization capacity of the water-pool decreases.

Buffer Solubility in PFPE-NH₄ Stabilized Microemulsions.

Table 1 presents a comparison of the maximum solubility of each buffer in the PFPE-NH₄ stabilized microemulsions. Theoretically determined ionic strengths inside the aqueous droplets of the w/c microemulsions are also shown at the solubilization capacity of the water-pool. For a buffer to be an effective proton shield inside a microemulsion droplet it must be located inside the "central" water-pool. The organic zwitterionic buffers investigated, such as MES and HEPES, are highly polar and highly charged molecules due to the presence of sulfonate groups (pK_a = 1.5). Accordingly, these buffers reside in the central water-pool of the microemulsion. In addition, the pK_a values of organic zwitterionic buffers are relatively insensitive to ionic strength effects.⁴³ For all of the inorganic buffers, excluding sodium bicarbonate, the acid and conjugate bases are highly hydrophilic, relatively small, and negatively charged. Therefore, it is safe to assume that these buffers are also confined to the central water-pool and have no tendency to adhere either to the hydrophobic parts of the surfactant or to the negatively charged headgroups.^{41–43,46,72} The organic zwitterionic buffer Tricine could possibly partition outside of the water-pool at a pH between 5 and 7, due to its carboxylic acid end group (pK_a \sim 5), as well as the inorganic

buffer sodium bicarbonate, which forms a neutral acid species. Sodium hydroxide was assumed to be fully dissociated inside the center of the w/c microemulsion.

The solubility of each buffer in the microemulsion droplet can be partially explained by consideration of their solubilities in bulk water.^{41,73} Sodium hydroxide has the highest solubility in bulk water at 10.5 mol kg⁻¹ (0 °C). Of all the compounds studied, sodium pyrophosphate has the lowest solubility in bulk water (0.01 mol kg⁻¹). Hence, solubilities inside the microemulsion droplet appear to mirror the solubilities of these buffers in bulk water.

Even though their bulk solubilities are similar, the solubilities of organic zwitterionic buffers in the microemulsion droplets are greater than their inorganic counterparts, except for NaOH. Therefore, ionic strength effects must limit buffer solubilization inside the water-pool. For example, the ionic strength inside the dispersed phase of a w/c microemulsion containing 1 mol kg⁻¹ HEPES and the indicator NPS is estimated to be \sim 1.84, at 35 °C and 345 bar. For 0.5 mol kg⁻¹ Na₂PO₄ under identical conditions, the ionic strength is 1.60 and at a concentration of 1 mol kg⁻¹ is 2.86. The PFPE-NH₄ microemulsion appears to be intolerant to ionic strengths much above 2.5.

The organic zwitterionic buffers CAPS, TES, and Tricine are much less soluble in the water-pool of the w/c microemulsion. It is possible that the hydroxymethyl groups of both TES and Tricine cause these buffers to partition outside the central water-pool, affecting droplet stability. Accordingly, the solubility of these buffers in the microemulsion will be lower than the other organic zwitterionic buffers that remain in the central water-pool. The cyclohexyl-containing moiety of CAPS may somehow contribute to its low solubility in the w/c microemulsion.

pH as a Function of Buffer Concentration. From experimental data, the most effective compounds for buffering the aqueous phase in the w/c microemulsions and the biphasic water-CO₂ systems are HEPES, Na₂OH₃, and NaOH. Figure 4a,b displays experimental pH results for the aqueous phase in both a w/c microemulsion and biphasic system buffered by HEPES and Na₂CO₃, respectively. The data clearly demonstrate that HEPES and Na₂CO₃ can successfully shift the aqueous phase pH in a w/c microemulsion from a value of approximately 3.2^{23,30,32,74} to pH values exceeding 6. Also, Figure 4c shows the principal result that the dispersed phase in a w/c microemulsions can be successfully buffered to pH 7 with NaOH. However, w/c microemulsions loaded with 1.5 mol kg⁻¹ NaOH were only stable at high pressures and over a narrow temperature window between 30 and 35 °C. A transparent w/c microemulsion cannot be formed if there are deviations from these experimental conditions (data not shown). Higher concentrations of NaOH could be loaded into the biphasic water-CO₂

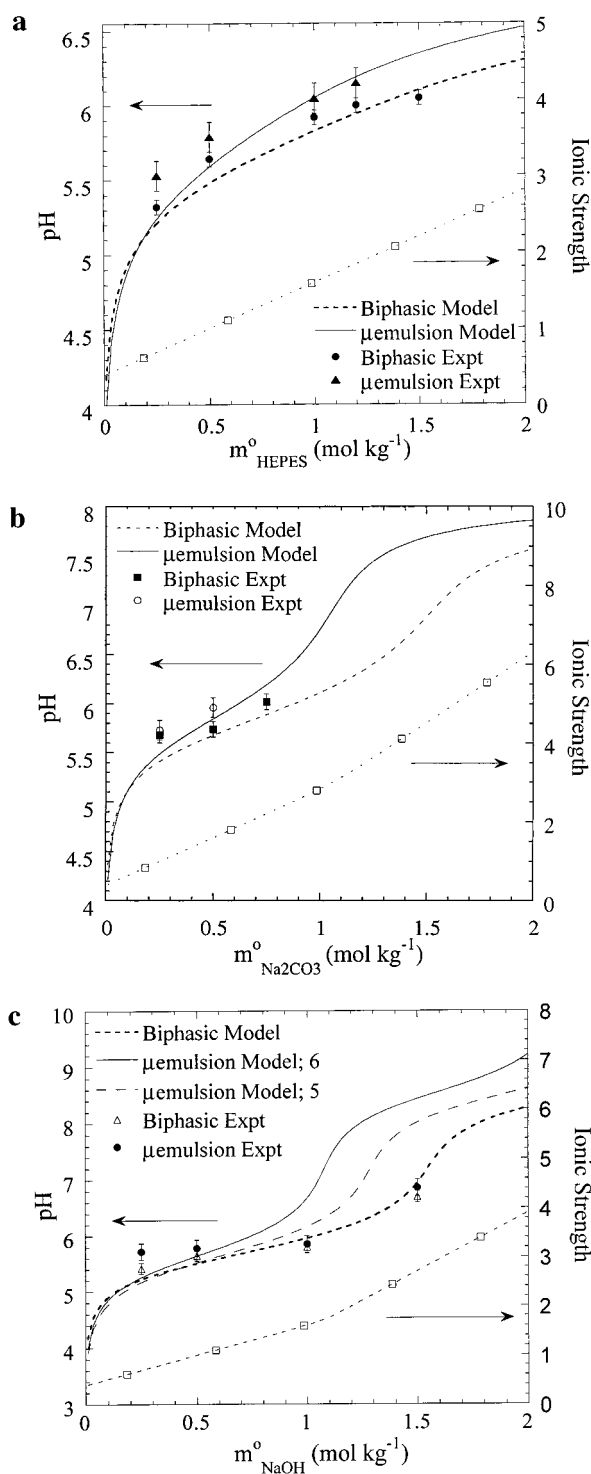


Figure 4. Experimentally and theoretically predicted aqueous pH results for w/c microemulsions and biphasic systems buffered with (a) HEPES, (b) Na₂CO₃, and (c) NaOH. In (c), the pH is predicted assuming either six or five bound water molecules per surfactant headgroup. Also shown are the predicted ionic strengths inside the w/c microemulsions as a function of buffer concentration. [NPS]_{aq} = 5 mmol kg⁻¹, *T* = 35 °C, and *P* = 345 bar.

experiments but unfortunately at these buffer concentrations NPS becomes insoluble and can no longer be used as an effective pH probe. Holmes et al.³⁰ have previously reported that 100 mmol kg⁻¹ MES solubilized in the aqueous phase of a di-HCF₄-stabilized microemulsion can fix the pH at approximately 5.2. Instability of the di-HCF₄ microemulsions at higher MES concentrations prevented the realization of much higher aqueous pH values.

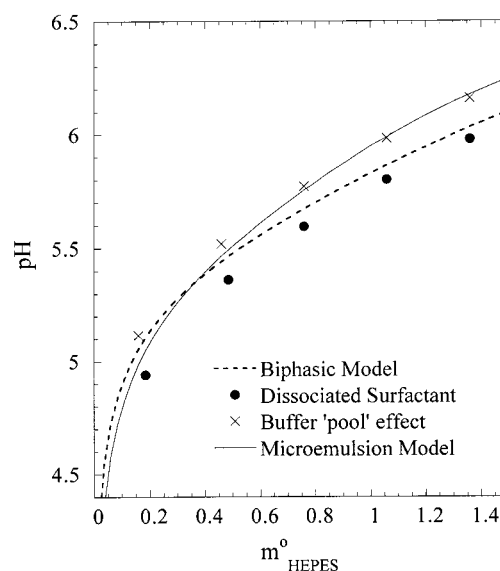


Figure 5. Predicted aqueous pH values inside a HEPES-buffered w/c microemulsion using the biphasic and microemulsion models. Also illustrated are how the predicted pH values differ from the biphasic model when accounting individually for buffer “pool” effects and changes in ionic strength due to dissociated surfactant molecules. *T* = 35 °C, *P* = 345 bar.

The theoretically predicted pH values calculated using the “biphasic” model are also shown in Figure 4. As a function of HEPES and Na₂CO₃ concentration, the biphasic model closely predicts the experimental pH values obtained for the water–CO₂ system at constant temperature and pressure. The experimental pH values for the w/c microemulsion are always higher than those predicted by the biphasic model. While this small deviation could be due to calibration error, any error associated with this method would only affect results at lower concentrations of buffer, i.e., below 0.5 mol kg⁻¹ and less, since the calibration curve would overpredict the ionic strength of the dispersed phase. Accurate pH prediction in a microemulsion, therefore, requires consideration of variables not observed in the biphasic water–CO₂ system, such as the structure of the water-pool^{30,61,75} and the ionic strength effects mentioned above. The water-pool in a w/o microemulsion can be divided into a “periphery” and a “central” part. Effective pH values in different regions of the reverse micelles have been calculated for AOT aggregates in heptane.^{43,50,61,72} Consequently, if we assume that six^{25,26,61,76} water molecules are associated with each PFPE-NH₄ headgroup and the buffer only resides in the “central” water-pool and does not partition into the “periphery” then at *w*₀ = 20, the concentration of the buffer in the water-pool will increase by a factor of 1.3:

$$m_{B,\text{microemulsion}}^o = 1.3m_{B,\text{bulk}}^o \quad (26)$$

Therefore, the “microemulsion model” predicts the aqueous phase pH in a w/c microemulsion, accounting for the environmental effects resulting from an increase in ionic strength and apparent buffer concentration.

Figure 5 illustrates how the predicted pH values differ from the “biphasic” model when accounting for buffer “pool effect” and ionic strength changes from dissociated surfactant headgroups and counterions. As seen in Figure 2, the ionic strength effect will lower the pH at a given buffer concentration while the “pool effect” will raise the pH due to an increase in the basic buffer concentration. Overall, the “microemulsion” model predicts that the aqueous pH inside the microemulsion droplet

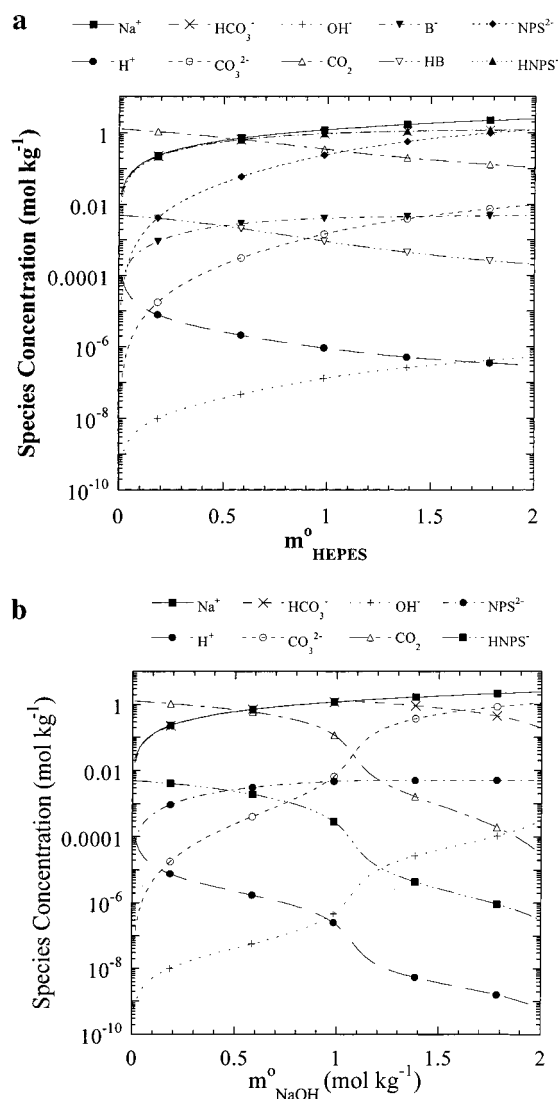


Figure 6. Speciation diagrams showing the change in molality of ionic species present in the aqueous phase of w/c microemulsions as a function of buffer concentrations: (a) [HEPES]_{aq}; (b) [NaOH]_{aq}. $T = 35\text{ }^{\circ}\text{C}$, $P = 345\text{ bar}$.

will be higher than anticipated by the biphasic model, as observed experimentally in Figure 4a,b.

Figure 4c shows the experimental and theoretical pH values for the w/c microemulsions and biphasic systems buffered with NaOH. For the microemulsion, there is a significant deviation between the experimental pH data and the values predicted using the microemulsion model. It is likely that the activity coefficient model becomes inaccurate at high NaOH concentrations. It is also possible that the number of water molecules associated with each PFPE-NH₄ head group, assumed to be six, may be inaccurate. Figure 4c also shows a dramatic decrease in the predicted aqueous pH values in a NaOH-buffered w/c microemulsion if five water molecules are assumed to be bound to each surfactant molecule. Alternatively, there may be some changes in the structural binding of water molecules to the surfactant headgroups in the presence of NaOH.

As anticipated, increasing the concentration of any of the buffers increases the pH of the aqueous phase in both the microemulsion and biphasic system. For the buffers studied a pH "jump" of between 2 and 2.5 pH units can be achieved at relatively low buffer concentrations. For example, when 0.25 mol kg⁻¹ HEPES, Na₂CO₃, and NaOH are dispersed in the w/c microemulsion the aqueous pH shifts from a value between 3

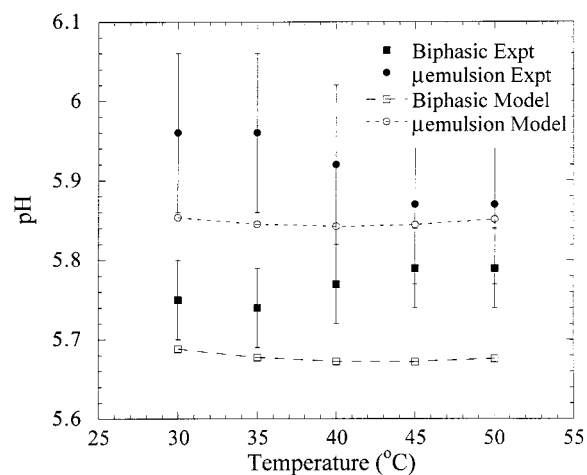


Figure 7. Experimentally and theoretically determined aqueous pH results for w/c microemulsions and biphasic systems buffered with Na₂CO₃ as a function of temperature. [Na₂CO₃]_{aq} = 0.5 mol kg⁻¹, [NPS]_{aq} = 5 mmol kg⁻¹, $P = 345\text{ bar}$.

and 3.2^{23,30} to pH values of 5.53, 5.68, and 5.72 (± 0.1), respectively. Increasing the aqueous buffer concentration further to 1.2 and 1.5 mol kg⁻¹ for HEPES and NaOH and 0.5 mol kg⁻¹ for Na₂CO₃ results in a further pH increase of 0.22, 0.62, and 1.14, respectively.

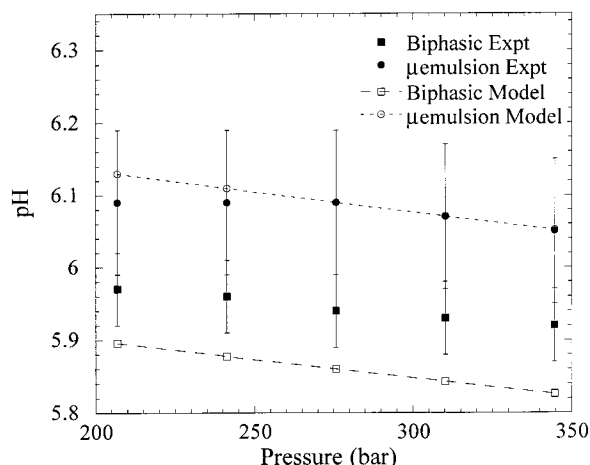
Figures 4 and 6 demonstrate how the concentrations of the individual ionic species and pH in the aqueous phase of the w/c microemulsions vary as a function of base concentration. The initial steep increase in pH with small buffer loadings results from the titration of aqueous CO₂ (or H₂CO₃ pK_{a1} 6.3) by the buffer. This reduction in the concentration of aqueous CO₂ results in a decrease in the concentration of protons and hence an initially pH "jump" followed by a plateau due to buffering from the carbonic acid–bicarbonate equilibrium, e.g., Figures 4a and 6a. As observed with stronger bases like NaOH in Figures 4c and 6b, another sharp increase in pH would be expected at a pH approaching 7 due to a significant rise in the concentration of CO₃²⁻ upon approaching pK_{a2} . This increase in the pH of the aqueous phase would be expected at greater buffer concentrations than those studied, since the carbonic acid–bicarbonate equilibrium dominates the behavior.

The variation in the ionic strength inside the aqueous phase of the w/c microemulsion for HEPES, Na₂CO₃, and NaOH is also presented in Figure 4. There is a linear increase in the ionic strength of the dispersed phase as a function of buffer concentration. Table 2 summarizes the experimentally and theoretically determined aqueous pH values for w/c microemulsions and biphasic systems loaded with various buffers.

pH as a Function of Temperature and Pressure. Figure 7 displays pH results for the aqueous phase in both a w/c microemulsion and biphasic system loaded with Na₂CO₃ (0.5 mol kg⁻¹) as a function of temperature. As predicted by the microemulsion and biphasic models, the pH data obtained for Na₂CO₃ appears to change very little with rising temperatures. The pH of the aqueous phase buffered with 100 mmol kg⁻¹ MES in a w/c microemulsion stabilized by the di-HCF₄ surfactant has been previously reported to increase by approximately 0.1 pH units between 15 and 30 $^{\circ}\text{C}$.³⁰ These trends were observed to mirror the solubility of CO₂ as a function of temperature.^{36,37} At this low buffer concentration, the pH change resulting from the decrease of CO₂ in the droplet dominates over the effects due to $d(pK_a)/dT$ and, therefore, the pH was

TABLE 2: Comparison of Experimentally and Theoretically Determined Buffered-Aqueous pH Values in w/c Microemulsions and Biphasic Water–CO₂ Systems, $T = 35\text{ }^{\circ}\text{C}$, $P = 345\text{ bar}$

buffer name	buffer concn (mol kg ⁻¹)	experimentally determined pH in biphasic water–CO ₂ system	experimentally determined aqueous pH in w/c microemulsion	predicted aqueous pH in bulk water–CO ₂ system	predicted aqueous pH in w/c microemulsion
CAPS	0.2	4.94	5.02	5.14	5.15
Na ₂ CO ₃	0.5	5.74	5.96	5.68	5.84
Na ₃ P ₂ O ₆	0.2	5.09	5.17	4.84	4.93
Tricine	0.8	5.58	5.51	5.75	6.00
HEPES	1.0	5.92	6.05	5.94	6.19
TES	0.5	5.42	5.61	5.47	5.57
BES	1.1	5.67	5.93	5.76	5.91
Na ₂ HPO ₄	0.5	5.14	5.18	5.12	5.14
NaHCO ₃	0.5	5.41	5.64	5.33	5.37
MES	1.0	5.49	5.76	5.38	5.42
NaOH	1.5	6.70	6.86	6.94	8.43

**Figure 8.** Experimentally and theoretically determined aqueous pH results for w/c microemulsions and biphasic systems buffered with HEPES as a function of pressure. $[\text{HEPES}]_{\text{aq}} = 1.0\text{ mol kg}^{-1}$, $[\text{NPS}]_{\text{aq}} = 5\text{ mmol kg}^{-1}$, $T = 35\text{ }^{\circ}\text{C}$.

observed to increase as a function of temperature. In the present study at higher buffer concentrations, the two effects compensate each other.

Figure 8 shows pH results for the aqueous phase in both a w/c microemulsion and biphasic system loaded with HEPES as a function of pressure. The solubility of CO₂ in aqueous solution increases as a function of pressure.^{36,37} This increase in the molality of CO₂ in the aqueous phase of bulk water or aqueous droplets in a w/c microemulsion will result in a very slight lowering of pH.³⁰ Table 3 summarizes the aqueous pH values obtained for a variety of buffers studied as a function of temperature and pressure. Small decreases in pH as a function of temperature and pressure are in agreement with the predicted trends.

Conclusions

The aqueous phase in PFPE-NH₄-stabilized microemulsions and biphasic water–CO₂ systems can be successfully buffered to pH values approaching 7. Inorganic and organic zwitterionic buffers and NaOH can be used to control the aqueous pH in these systems over a pH range between 3 and values from 5 to 7. For the w/c microemulsion and biphasic systems studied, an initial pH “jump” was observed with small buffer loadings resulting from the titration of carbonic acid with the alkaline buffers. Large amounts of base are required to further increase pH due to the buffer capacity of the carbonic acid–bicarbonate equilibrium; values approaching 7 were obtained with NaOH.

The solubility of each buffer in the w/c microemulsion mirrors its solubility in bulk water, although ionic strength effects and

TABLE 3: Summary of the Aqueous pH Values Obtained Experimentally for a Variety of Buffers Studied as a Function of Temperature and Pressure

buffer	temp (°C)	pressure (bar)	biphasic pH	microemulsion pH
Na ₂ CO ₃ (0.5 mol kg ⁻¹)	30	345	5.75	5.96
	50	345	5.79	5.87
	35	207	5.80	5.90
	35	310	5.75	5.88
Tricine (0.8 mol kg ⁻¹)	30	345	5.57	5.49
	50	345	5.63	5.55
	35	207	5.57	5.53
	35	310	5.58	5.48
HEPES (1 mol kg ⁻¹)	30	345	5.95	6.05
	50	345	5.91	6.15
	35	207	5.97	6.09
	35	310	5.93	6.07
BES (1 mol kg ⁻¹)	30	345	5.67	5.90
	50	345	5.65	5.84
	35	207	5.65	5.94
	35	310	5.61	5.90
NaHCO ₃ (0.5 mol kg ⁻¹)	30	345	5.41	5.63
	50	345	5.45	5.66
	35	207	5.42	5.67
	35	310	5.40	5.65
MES (1 mol kg ⁻¹)	30	345	5.49	5.76
	50	345	5.49	5.73
	35	207	5.49	5.73
	35	310	5.50	5.76
NaOH (1 mol kg ⁻¹)	30	345	5.76	5.83
	50	345	5.82	5.87
	35	207	5.84	5.91
	35	310	5.85	5.88
NaOH (1.5 mol kg ⁻¹)	30	345	6.67	6.62
	35	345	6.70	6.86

the partitioning of the compound out of the central water-pool also affect solubility. The w/c microemulsions stabilized by PFPE-NH₄ ($M_w = 672$) showed instability at ionic strengths at and above 1.6.

Under similar conditions the aqueous phase pH values observed in w/c microemulsions are always higher than those measured in biphasic water–CO₂ systems. This result reflects the environmental differences between biphasic water and water dispersed in w/c microemulsions, in particular, the binding of water molecules to surfactant headgroups in the microemulsion, which raises the buffer concentration. The dependence of the experimental aqueous pH in both the w/c microemulsions and biphasic systems on temperature and pressure was discovered to be insignificant.

Finally, the aqueous phase pH in biphasic water–CO₂ and PFPE-NH₄-stabilized microemulsions can be predicted with thermodynamic models based on knowledge of CO₂ solubility in water, and the relevant equilibrium constants. The pH values

in the microemulsions can be predicted reasonably well, to within 0.5 units, with the simple biphasic model for bulk systems without any surfactant present. Further accuracy is obtained with a microemulsion model by including changes due to the dissociation and hydration of surfactant head groups. The ability to successfully control and predict the pH inside w/c microemulsions is of fundamental importance for applications including catalytic reactions, enzymatic bioconversions, and extraction processes.

Acknowledgment. We acknowledge support from NSF (CTS-9626828), DOE (DE-FG03-96ER14664), the Texas Advanced Technology Program, and the Separations Research Program at the University of Texas. J.D.H. would like to thank Dr. Tamsin Mansley for her help with the synthesis and characterization of the indicator NPS.

References and Notes

- (1) Gonzalez, A.; Murphy, J.; Holt, S. L. In *Chemical Reactions in Water-in-Oil Microemulsions*; Holt, S. L., Ed.; American Chemical Society: Washington, DC, 1982; pp 165.
- (2) Martin, C. A.; McCrann, P. M.; Angelos, G. H.; Jaeger, D. A. *Tetrahedron Lett.* **1982**, 23, 4651.
- (3) Menger, F. M.; Rhee, J. U.; Rhee, H. K. *J. Org. Chem.* **1975**, 40, 3803.
- (4) Pileni, M. P. *J. Phys. Chem.* **1993**, 97, 6961.
- (5) Gargouri, M.; Drouet, P.; Hervagault, J. F.; Legoy, M. D. *Biotech. Bioeng.* **1996**, 51, 573.
- (6) Jenta, T. R.-J.; Batts, G.; Rees, G. D.; Robinson, B. H. *Biotech. Bioeng.* **1997**, 54, 416.
- (7) Luisi, P. L.; Meier, P.; Imre, V. E.; Pande, A. In *Enzymes and Nucleic Acids Solubilized in Hydrocarbon Solvents with the Help of Reverse Micelles*; Luisi, P. L., Straub, B. E., Eds.; Plenum Press: New York, 1982; Vol. 1, pp 323.
- (8) Rees, G. D.; Katherine, C.; Crooks, G. E.; Jenta, T. R.-J.; Price, L. A.; Robinson, B. H. In *Lipases in Water-in-Oil Microemulsions, Organogels and Winsor II Systems: Aspects of Reactivity and Separation Science*; Maccata, F. X., Ed.; Kluwer Academic Publishers: 1996; pp 577.
- (9) Wold, F. In *Enzymes*; Hager, L., Wold, F., Eds.; Prentice-Hall Inc.: Englewood Cliffs, NJ, 1971; pp 53.
- (10) Yamada, Y.; Kuboi, R.; Komasa, I. *J. Chem. Eng. Jpn.* **1994**, 27, 404.
- (11) Göklen, K. E.; Hatton, T. A. *Biotechnol. Prog.* **1985**, 1, 69.
- (12) Gupta, R. B.; Han, C. J.; Johnston, K. P. *Biotechnol. Bioeng.* **1994**, 44, 830.
- (13) Vasudevan, M.; Wieneck, J. M. *Ind. Eng. Chem. Res.* **1996**, 35, 1085.
- (14) Tondre, C.; Hebrant, M.; Perdicakis, M.; Bessiere, J. *Langmuir* **1997**, 13, 1446.
- (15) Motte, L.; Petit, C.; Boulanger, L.; Lixon, P.; Pileni, M. P. *Langmuir* **1992**, 8, 1049.
- (16) Peral, J.; Mills, A. J. *Photochem. Photobiol. A* **1993**, 73, 47.
- (17) Pileni, M. P.; Motte, L.; Petit, C. *Chem. Mater.* **1992**, 4, 338.
- (18) Pileni, M. P. *Langmuir* **1997**, 13, 3266.
- (19) Towey, T. F.; Khan-Lodhi, A.; Robinson, B. H. *J. Chem. Soc., Faraday Trans.* **1990**, 86, 2757.
- (20) Lisiecki, I.; Bjorling, M.; Motte, L.; Ninham, B.; Pileni, M. P. *Langmuir* **1995**, 11, 2385.
- (21) Feltin, N.; Pileni, M. P. *Langmuir* **1997**, 13, 3927.
- (22) McHugh, M. A.; Krukons, V. J. *Supercritical Fluids Extraction: Principles and Practice*, 2nd ed.; Butterworth-Heinemann: Boston, MA, 1993.
- (23) Niemeyer, E. D.; Bright, F. V. *J. Phys. Chem.* **1998**, 102, 1474.
- (24) Zielinski, R. G.; Kline, S. R.; Kaler, E. W.; Rosov, N. *Langmuir* **1997**, 13, 3934.
- (25) Heitz, M. P.; Carlier, C.; deGrazia, J.; Harrison, K. L.; Johnston, K. P.; Randolph, T. W.; Bright, F. V. *J. Phys. Chem.* **1997**, 101, 6707.
- (26) Johnston, K. P.; Harrison, K.; Clarke, M. J.; Howdle, S. M.; Heitz, M. P.; Bright, F. V.; Carlier, C.; Randolph, T. W. *Science* **1996**, 271, 624.
- (27) Harrison, K. L.; Goveas, J.; Johnston, K. P.; O'Rear, E. A., III, *Langmuir* **1994**, 10, 3536.
- (28) Eastoe, J.; Bayazit, Z.; Martel, S.; Steytler, D. C.; Heenan, R. K. *Langmuir* **1996**, 12, 1423.
- (29) Eastoe, J.; Cazelles, B. M. H.; Steytler, D. C.; Holmes, J. D.; Pitt, A. R.; Wear, T. J.; Heenan, R. K. *Langmuir* **1997**, 13, 6980.
- (30) Holmes, J. D.; Steytler, D. C.; Rees, G. D.; Robinson, B. H. *Langmuir* **1998**, 14, 6371.
- (31) Clarke, M. J.; Harrison, K. L.; Johnston, K. P.; Howdle, S. M. *J. Am. Chem. Soc.* **1997**, 119, 6399.
- (32) Toews, K. L.; Shroll, R. M.; Wai, C. M.; Smart, N. G. *Anal. Chem.* **1995**, 67, 4040.
- (33) Fletcher, P. D. I.; Robinson, B. H.; Freedman, R. B.; Oldfield, C. *J. Chem. Soc., Faraday Trans. 1* **1985**, 81, 2667.
- (34) Ashraf-Khorassani, M.; Combs, M. T.; Taylor, L. T. *J. Chromatogr. A* **1997**, 774, 37.
- (35) Atkins, P. W. *Physical Chemistry*, 3rd ed.; Oxford University Press: Oxford, U.K., 1987.
- (36) Wiebe, R.; Gaddy, V. L. *J. Am. Chem. Soc.* **1941**, 63, 475.
- (37) Wiebe, R. *Chem. Rev.* **1941**, 29, 475.
- (38) King, M. B.; Mubarak, A.; Kim, J. D.; Bott, T. R. *J. Supercrit. Fluids* **1992**, 5, 296.
- (39) Beynon, R. J.; Easterby, J. S. *Buffer Solutions*, 1st ed.; Oxford University Press: New York, 1996.
- (40) Ferguson, W. J.; Braunschweiger, K. I.; Braunschweiger, W. R.; Smith, J. R.; McCormick, J. J.; Wasmann, C. C.; Jarvis, N. P.; Bell, D. H.; Good, N. E. *Anal. Biochem.* **1980**, 104, 300.
- (41) Good, N. E.; Winget, G. D.; Winter, W.; Connolly, T. N.; Izawa, S.; Singh, R. M. M. *Biochemistry* **1966**, 5, 467.
- (42) Good, N. E.; Izawa, Z. *Methods Enzymol., Part B* **1972**, 14, 53.
- (43) Oldfield, C.; Robinson, B. H.; Freedman, R. B. *J. Chem. Soc., Faraday Trans.* **1990**, 86, 833.
- (44) El Seoud, O. A.; Chinelatto, A. M.; Shimizu, M. R. *J. Colloid Interface Sci.* **1982**, 88, 420.
- (45) El Seoud, O. A.; Chinelatto, A. M. *J. Colloid Interface Sci.* **1983**, 95, 163.
- (46) Fujii, H.; Kawai, T.; Nishikawa, H.; Ebert, G. *Colloid Polym. Sci.* **1982**, 260, 697.
- (47) Terpko, A. T.; Serafin, R. J.; Bucholtz, M. L. *J. Colloid Interface Sci.* **1981**, 84, 202.
- (48) Reinsborough, V. C.; Holzwarth, J. F. *Can. J. Chem.* **1986**, 64, 955.
- (49) Wormuth, K. R.; Cadwell, L. A.; Kaler, E., W. *Langmuir* **1990**, 6, 1035.
- (50) Menger, F. M.; Saito, G. *J. Am. Chem. Soc.* **1978**, 100, 4376.
- (51) Hornbeck, R. W. *Numerical Methods*, 1st ed.; Prentice-Hall: Englewood Cliffs, NJ, 1975.
- (52) Stumm, W.; Morgan, J. J. *Aquatic Chemistry: Chemical Equilibria and Rates in Natural Waters*, 3rd ed.; John Wiley & Sons, Inc.: New York, 1996.
- (53) Marshall, W. L.; Franck, E. U. *J. Phys. Chem. Ref. Data* **1981**, 10, 1.
- (54) Pitzer, K. S. *Activity Coefficients in Electrolyte Solutions*; CRC Press: Boca Raton, FL, 1991; p 75.
- (55) Oscarson, J. L.; Gillespie, S. E.; Izatt, R. M.; Chen, X.; Pando, C. *J. Solution Chem.* **1992**, 21, 789.
- (56) Caporiccio, G.; Burzio, F.; Carniselli, G.; Biancardi, V. *J. Colloid Interface Sci.* **1984**, 98, 202.
- (57) Schiers, J. *Perfluoropolyethers (Synthesis, Characterization and Applications)*, 1st ed.; Schiers, J., Ed.; John Wiley & Sons Ltd: London, 1997.
- (58) Shugar, G. J.; Dean, J. D. *The Chemist's Ready Reference Handbook*; McGraw-Hill Inc.: New York, 1990.
- (59) Vogel, A. I. *Vogel's Textbook of Practical Organic Chemistry, Including Qualitative Organic Analysis*, 4th ed.; Longman Press: London, 1978.
- (60) McFann, G. J.; Johnston, K. P.; Howdle, S. M. *AIChE J.* **1994**, 40, 543.
- (61) El Seoud, O. A. In *Acidities and Basicities in Reversed Micellar Systems*, 1st ed.; Luisi, P. L., Straub, B. E., Eds.; Plenum Press: New York, 1984.
- (62) Huang Kenez, P.; Carlstrom, G.; Furo, I.; Halle, B. *J. Phys. Chem.* **1992**, 96, 9524.
- (63) Toullec, J.; Couderc, S. *Langmuir* **1997**, 13, 1918.
- (64) Romsted, I. S.; Yoon, C.-O. *J. Am. Chem. Soc.* **1993**, 115, 989.
- (65) Hou, M.-J.; Shah, D. O. *Langmuir* **1987**, 3, 1086.
- (66) Leung, R.; Shah, D. O. *J. Colloid Interface Sci.* **1987**, 120, 320.
- (67) Leung, R.; Shah, D. O. *J. Colloid Interface Sci.* **1987**, 120, 330.
- (68) Jada, A. J.; Zana, R. *J. Phys. Chem.* **1990**, 94, 381.
- (69) Peck, D. G.; Johnston, K. P. *J. Phys. Chem.* **1991**, 95, 9549.
- (70) Peck, D. G.; Mehta, A. J.; Johnston, K. P. *J. Phys. Chem.* **1989**, 93, 4297.
- (71) Jacobson, G. B.; Lee, C. T., Jr.; Johnston, K. P. *J. Org. Chem.* **1999**, 64, 1201.
- (72) Fujii, H.; Kawai, T.; Nishikawa, H. *Bull. Chem. Soc. Jpn.* **1979**, 52, 2051.
- (73) Weast, R. C. *CRC Handbook of Chemistry and Physics*, 54th ed.; CRC Press: Cleveland, OH, 1973.
- (74) Crovetto, R.; Wood, R. H.; Majer, V. *J. Chem. Thermodyn.* **1990**, 22, 231.
- (75) El Seoud, O. A.; Shimizu, M. R. *Colloid Polym. Sci.* **1982**, 260, 794.
- (76) De, T. K.; Maitra, A. *Adv. Colloid Interface Sci.* **1995**, 59, 95.